Structure and hydrogen bond dynamics of water–dimethyl sulfoxide mixtures by computer simulations

Alenka Luzar[a] and David Chandler
Department of Chemistry, University of California, Berkeley, Berkeley, California 94720

(Received 21 December 1992; accepted 26 January 1993)

We have used two different force field models to study concentrated dimethyl sulfoxide (DMSO)–water solutions by molecular dynamics. The results of these simulations are shown to compare well with recent neutron diffraction experiments using H/D isotope substitution [A. K. Soper and A. Luzar, J. Chem. Phys. **97**, 1320 (1992)]. Even for the highly concentrated 1 DMSO : 2 H_2O solution, the water hydrogen–hydrogen radial distribution function, $g_{HH}(r)$, exhibits the characteristic tetrahedral ordering of water–water hydrogen bonds. Structural information is further obtained from various partial atom–atom distribution functions, not accessible experimentally. The behavior of water radial distribution functions, $g_{OO}(r)$ and $g_{OH}(r)$ indicate that the nearest neighbor correlations among remaining water molecules in the mixture increase with increasing DMSO concentration. No preferential association of methyl groups on DMSO is detected. The pattern of hydrogen bonding and the distribution of hydrogen bond lifetimes in the simulated mixtures is further investigated. Molecular dynamics results show that DMSO typically forms two hydrogen bonds with water molecules. Hydrogen bonds between DMSO and water molecules are longer lived than water–water hydrogen bonds. The hydrogen bond lifetimes determined by reactive flux correlation function approach are about 5 and 3 ps for water–DMSO and water–water pairs, respectively, in 1 DMSO : 2 H_2O mixture. In contrast, for pure water, the hydrogen bond lifetime is about 1 ps. We discuss these times in light of experimentally determined rotational relaxation times. The relative values of the hydrogen bond lifetimes are consistent with a statistical (i.e., transition state theory) interpretation.

I. INTRODUCTION

Dimethyl sulfoxide (DMSO), $(CH_3)_2SO$, is an important industrial solvent as well as being used widely in biology as a cryoprotector in the denaturation of proteins, and as a drug carrier across cell membranes.[1] Unquestionably the broad range of properties are closely related to its properties in water solutions. The partial negative charge on the oxygen atom of the DMSO molecule favors the formation of the hydrogen bonds with water molecules, giving rise to strongly nonideal behavior of the mixture. A solution of 1 mol DMSO to ~3 mol H_2O has a freezing point of −70 °C compared to +18.6 and 0 °C for the pure constituents, respectively.[2] The nonideality of the variation of the dielectric constant with composition[3,4] is paralleled by similar positive deviations of the viscosity and density[5] and negative deviations of heats of mixing.[5–8] The maximum deviations occur at 30–40 mol % of DMSO. One might expect that strong associates like DMSO–2 H_2O exist in the region of extrema of the excess quantities. The existence of well defined complexes of this composition has, however, not so far been proved.

In earlier work[9–11] an attempt was made to analyze thermodynamic properties of the mixture in a mean-field approximation. A simple model for hydrogen bonded solution was shown to describe the experimental data for the excess enthalpies and free energies of mixing, as well as the excess surface free energies of mixing reasonably well over the entire composition range. The model accounts for only the hydrogen bond interaction between molecules, suggesting a nearly tetrahedral hydrogen bonding complex involving two or three water molecules per DMSO molecule. The same simplified description of the hydrogen bond interaction has also been capable of predicting the observed dielectric behavior.[12] While the success of the model would indicate the dominant role of hydrogen bond interaction in this mixture, the model does not provide the answer to what is the geometrical arrangement of water molecules neighboring DMSO in the solution. Also, the degree to which the coordination of DMSO by water can be regarded as a long lived complex is not known.

Very little consensus among experimentalists exists[5,13–17] regarding these questions. Controversy arises primarily because the techniques that are used, such as measurements of thermodynamic quantities,[4–8] measurements of excitation spectra via IR absorption,[17,18] Raman scattering,[17] or NMR (nuclear magnetic resonance),[19–21] as well as inelastic neutron and x-ray scattering[13] are either not sensitive to the detailed microscopic structure or else require a considerable degree of interpretation to obtain structural information. Recent advances in neutron diffraction techniques[22] allow the hydrogen bonding geometry to be probed directly in the solution, through the use of iso-

[a]Also affiliated with Medical Faculty and Josef Stefan Institute, University of Ljubljana, Slovenia.

 0021-9606/93/108160-14$06.00

tope substitutions[23] which can determine separate atom–atom distribution functions. The results of the neutron experiment can be less susceptible to erroneous model interpretation than the above mentioned techniques.

Recently, one of us[24] has performed a neutron diffraction experiment with H/D isotope substitution, the first on the DMSO–water system, on small angle neutron diffractometer for amorphous and liquid samples (SANDALS) at the ISIS pulsed neutron source at Rutherford Appleton Laboratory, which is optimized for diffraction studies of materials with light atoms. The DMSO was deuterated in the experiment to reduce the large level of incoherent scattering by protons as much as possible. We have looked at two concentrated DMSO–water solutions, one at roughly 1 DMSO : 2 H_2O, corresponding to minima or maxima in several thermodynamic properties,[4–8] and the other at roughly 1 DMSO : 4 H_2O in order to investigate the trend with dilution. These concentrations also straddle the composition at which DMSO forms a stable hydrate in the crystalline state, 1 DMSO : 3 H_2O.[2]

Terms like "enhancement" and "breakdown" of water structure have frequently been applied to different solutes, including DMSO dissolved in water. There is a degree of ambiguity in this terminology as the conclusions drawn depend upon which physical properties are observed. The neutron scattering data[24] show that the most probable local water structure is not strongly affected by the presence of DMSO in the sense that the peak locations of the first molecular coordination shell are preserved at both concentrations studied. As expected on simple geometrical grounds,[9–11] one does observe a reduction of the H–H coordination number with increasing concentration of DMSO. The percentage of water molecules that are hydrogen bonded to themselves in this manner is substantially reduced compared to pure water, because an increasing fraction of water molecules are bonded to DMSO. The trend in coordination number with concentration agrees with that predicted by the simple hydrogen bonding model for DMSO–water solutions given in Refs. 9–11.

The neutron diffraction experiment result that DMSO does not disrupt the most probable geometry of the first molecular coordination shells but does alter the likelihood of such hydrogen bonding structures forming in the liquid is not inconsistent with, for example, Baker and Jonas' observations.[21] They found that that the pressure anomaly in H_2O self-diffusion disappears for DMSO concentrations of the order of or higher than mole fraction 0.2. Evidently, while DMSO at those concentrations may not destroy the local tetrahedral structure, it does destroy the extension of the tetrahedral networks in water beyond the first coordination shell. This interpretation would also explain the large depression in freezing point for the liquid. To make the interpretation quantitative, it now seems appropriate to carry out detailed computer simulation involving reasonably realistic potentials for the DMSO–water system. We have chosen to perform molecular dynamics (MD) computer simulations to interpret the neutron diffraction data[24] and to offer additional insight, as well as to help to check the accuracy of the already existing phenomenological model of hydrogen-bonded mixtures.[9–12] The MD allows us to compute quantities of relevance to the phenomenology, such as maximum numbers of hydrogen bonds between water and DMSO molecules, but not directly accessible from experiment. In this paper we report such calculation on DMSO–water mixture at two concentrations that were used in the neutron diffraction experiment.[24] Using a different potential model than we adopt, Vaisman and Berkowitz have recently reported molecular dynamics results for water–DMSO mixtures at low DMSO concentrations.[25]

The rest of the paper is organized as follows: In Sec. II the potential models and technical details of the MD calculations are described. In Sec. III the structure of the mixture is discussed on the basis of various radial distribution functions and the geometric arrangements of nearest neighbors. First the partial correlation functions obtained from the simulations are presented. Further the comparison with neutron diffraction data is given, in terms of hydrogen–hydrogen radial distribution function, $g_{HH}(r)$, between water protons and so bares a direct relation to the same quantity in pure water. Hydrogen bonding analysis is further carried out by comparing the coordination numbers estimated from experiment[24] and those estimated from mean-field-type model.[9] In Sec. IV we present a preliminary analysis of the hydrogen bond dynamics, based on the reactive flux correlation function approach.[26–28] Hydrogen bond lifetimes for water–water and water–DMSO interaction in the mixture are estimated and compared with hydrogen bond lifetimes, calculated for pure water. Conclusions are found in Sec. V.

II. POTENTIALS AND METHOD

The interactions between water and DMSO molecules were assumed to be composed of pairwise additive potential functions between atomic sites. For water–water interactions, we used the simple-point-charge (SPC) model of Berendsen *et al.*[29] For DMSO, we chose to construct our own potential because the only one available in the literature so far,[25,30] gives not entirely accurate thermodynamics.[31]

The intermolecular DMSO–water potential is represented as a sum of pairwise Coulomb and 6–12 Lennard-Jones:

$$u_{\alpha\beta}(r)=\frac{q_\alpha q_\beta}{r}+4\epsilon_{\alpha\beta}\left[\left(\frac{\sigma_{\alpha\beta}}{r}\right)^{12}-\left(\frac{\sigma_{\alpha\beta}}{r}\right)^{6}\right], \tag{1}$$

where α and β denote a pair of interaction sites on different molecules, r is the site–site separation, q_α is a point charge located at site α, and $\epsilon_{\alpha\beta}$ and $\sigma_{\alpha\beta}$ are the energy and distance parameters in the Lennard-Jones potential. Cross interactions were obtained from Lorentz–Berthelot rule

$$\sigma_{\alpha\beta}=\tfrac{1}{2}(\sigma_{\alpha\alpha}+\sigma_{\beta\beta}), \quad \epsilon_{\alpha\beta}=(\epsilon_{\alpha\alpha}\epsilon_{\beta\beta})^{1/2}. \tag{2}$$

Our choice of the water–DMSO potential is consistent with the usual combining rules used in the statistical mechanics of mixtures[34] and with the independent determination of the intermolecular DMSO–DMSO and water–

TABLE I. Intermolecular potential parameters

	Water(SPC, Ref. 29)[a]		
	ϵ/kJ mol^{-1}	σ/Å	q
Oxygen	0.6502	3.1560	−0.82
Hydrogen	0.0	0.0	0.41

	DMSO[b]			
	ϵ/kJ mol^{-1}	σ/Å	q (P1 potential)	q (P2 potential)
Oxygen	0.29922	2.8	−0.54	−0.459
Sulphur	0.99741	3.4	0.54	0.139
Methyl group	1.230	3.8	0.0	0.160

[a]For the geometry of H_2O, we have taken the O–H bond length as 1 Å; and the HOH angle as 109.28°.
[b]For the geometry of DMSO, from Ref. 36, we used the S–O bond length of 1.53 Å, the S–C bond length of 1.8 Å, the OSC angle of 106.75°; and the CSC angle 97.4°.

water potentials. No parameter optimization has been carried out for mixtures, once the parameters for the pure compounds have been determined. This approach is a standard first approximation. Klein and co-workers[35] have shown it to be reasonably accurate for simulating water–methanol, water–acetone, and water–ammonia mixtures.

Both types of molecules in our simulation were modeled as completely rigid. The methyl groups on DMSO were replaced by united atoms of atomic mass 15. We have taken the intramolecular structure of DMSO from the crystallographic data.[36] The Lennard-Jones interaction coefficients and charges were chosen on the basis of experimentation with ~50 simulation runs, using as criteria accurate values for the heat of vaporization, vanishing pressure, and a molecular dipole moment at least as large as that of the gas phase molecule (~4 D).[37] The two model potentials, P1 and P2, used further in the simulation of the mixture, were chosen according to the best agreement with recent neutron diffraction data on pure DMSO (Ref. 38) and at the same time giving reasonably accurate values for the mean potential energy and pressure. In both models, the Lennard-Jones parameters for O, S, and CH_3 in DMSO are those of the isoelectronic Ne, Ar, and CH_4, respectively. In one of the models, P1, there are no charges on methyl groups. In the other model, P2, we used the partial point charges for DMSO obtained by fitting the electrostatic potential around this molecule.[39] A detailed discussion on the parameterization of the DMSO potential will be presented elsewhere.[38] All Lennard-Jones parameters and the fractional charges for water and DMSO are listed in Table I.

The number of particles in the simulation box was 250 for pure water, and for pure DMSO with the P2 potential. There were 432 particles in the simulations of pure DMSO with the P1 potential. Along with the pure liquids, we have studied two systems coinciding with the 1:1.85 and 1:3.7 DMSO–water mixtures. The first includes 162 water molecules and 88 DMSO molecules (corresponding to the higher concentration of the mixture measured with neutron diffraction[24]); the second includes 197 water molecules and 53 DMSO molecules (corresponding to the lower experimental concentration). In many cases we have carried out simulations first with the DMSO potential model P1, and second with the DMSO potential model P2. The calculation began with the molecules in a body centered cubic lattice, with a lattice constant of 24.564 Å (for 1:2 mixture) or 22.784 Å (for 1:4 mixture), which is consistent with the experimental room temperature densities.[5] The molecular dynamics calculations were carried out in N,V,T ensemble, and the Nosé–Hoover thermostat[40,41] was used to control the temperature at 298 K. The thermostat was switched off when calculating dynamic properties. The equations of motions were integrated using the velocity predictor–corrector method usually with a time step of 1.0 or 1.5 fs. Energy drift was 0.0023 kJ/mol per ps, which represents only 0.005% of the total energy. The long range electrostatic interactions were treated using Ewald summation technique.[42] Periodic boundary conditions were used together with the minimum image convention for non-Coulombic interactions.[42] All the simulations were extended up to 160 ps, where the first 50 ps were considered as equilibration. The runs were performed on a Cray XMP/416 and/or IBM/RS 6000. Results of the mean potential energy per mole, $\langle U\rangle$, and pressure P, together with the experimental estimates of $\langle U\rangle$,[33,43,44] are given in Table II.

TABLE II. Molecular dynamics results for DMSO aqueous mixtures; mean potential energy per mole, $\langle u\rangle$, and pressure p, using P1 potential or P2 potential for DMSO. Numbers in parentheses are the experimental estimates of the mean potential energy per mole (Ref. 33).

	With P1 potential		With P2 potential	
Mole fraction of DMSO	$-\langle U\rangle$/kJ mol^{-1}	P/kbars	$-\langle U\rangle$/ kJ mol^{-1}	P/kbars
0.21	47.90±0.4 (45.25)	0.39±0.5	47.90±0.4	0.41±0.5
0.35	50.87±0.5 (47.18)	0.30±0.5	49.90±0.4	0.41±0.5

III. STRUCTURAL RESULTS

A. Partial correlation functions

Atom–atom distribution functions $g_{\alpha\beta}(r)$ provide a good method to discuss the structure. In Figs. 1–5 we display all partial correlation functions for two potential models for DMSO used in the simulation of the mixture at the concentration 2 H_2O :1 DMSO. The largest differences between the two models are observed in the three out of six correlation functions involving O, S, and C of the DMSO molecule (Fig. 1). In contrast, the change from P1 to P2 produces no significant differences in the radial distribution functions for water molecules in the mixture (Fig. 2). Maxima of the first molecular coordination shell peaks for the radial distributions illustrated in Fig. 3 indicate that the nearest water molecules are hydrogen bonded to the oxygen in DMSO molecule.

DMSO is a suitable solvent to study small length scale manifestations of hydrophobicity as it has methyl groups which bear no strong interaction with water. The upper two curves in Fig. 4 show the distribution functions that

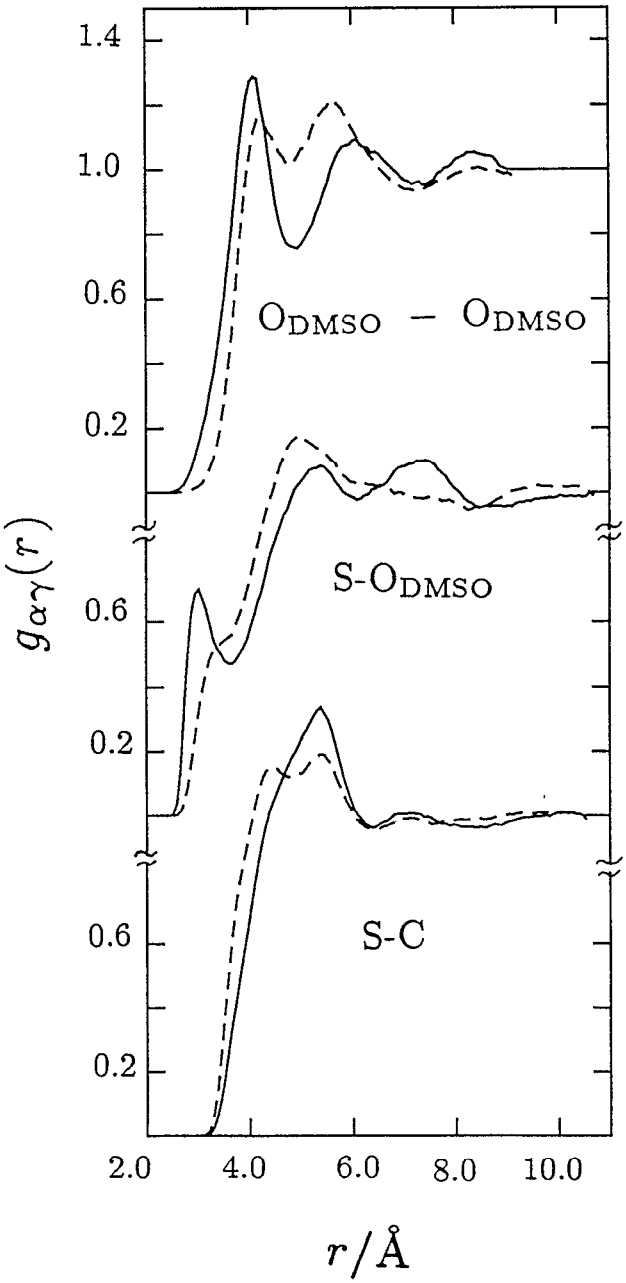

FIG. 1. Atom–atom distribution functions between pairs of DMSO molecules for water–DMSO mixture with DMSO mole fraction $x_2=0.35$. Full lines correspond to calculations using the P1 potential for DMSO and dotted lines correspond to calculations using P2 potential for DMSO. Capital letters indicate which pairs of atoms coincide with α and γ. All $g_{\alpha\gamma}(r)$'s are asymptotic to 1 at large r.

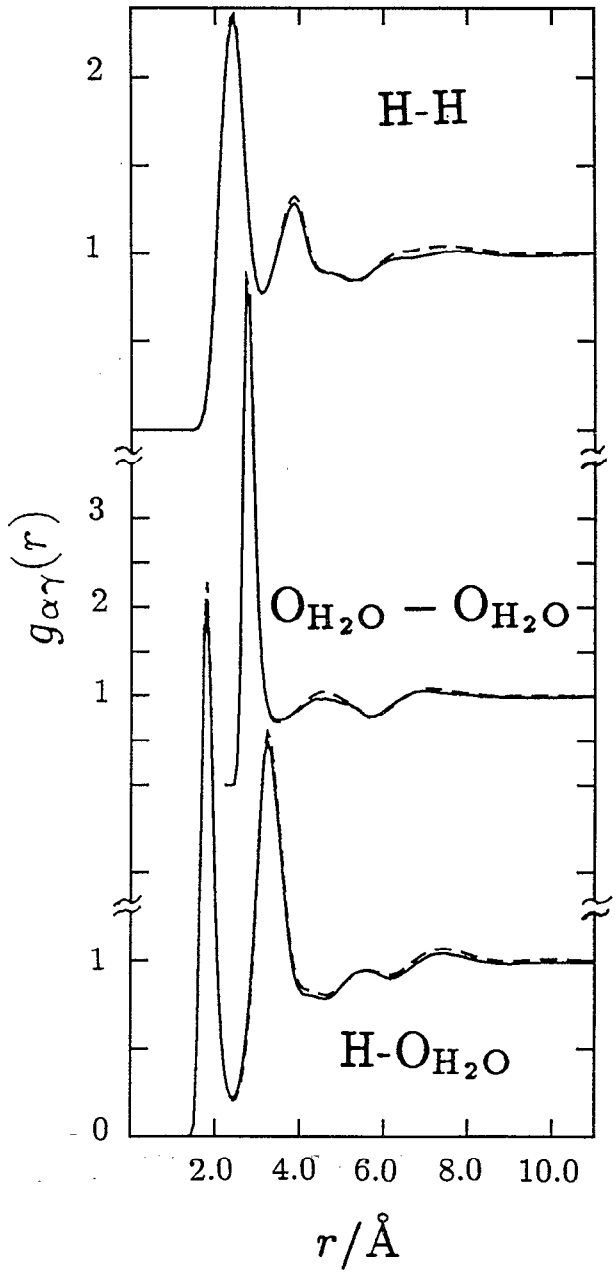

FIG. 2. Atom–atom pair distribution functions between pairs of water molecules for water–DMSO mixture with $x_2=0.35$. Lines and lettering as in Fig. 1. Note change of scale in middle panel.

characterize the radial hydration of methyl groups on DMSO. The lower two curves on Fig. 4 show the carbon–carbon distribution describing hydrophobic pair correlations of DMSO in the mixture. The first of them indicate that there are on the average 6.2 water oxygens around carbon within a 5.1 Å radius, the carbon–carbon function indicates that the carbon in the methyl group is surrounded by ~4.8 other carbon atoms within the same distance range. As the ratio of those two coordination numbers is not very different from the ratio of corresponding atomic fractions in the solution, hydrophobic association, if it exists among the methyl groups, does not seem to have a significant effect upon the structure of the mixture. It is interesting to note that these pair correlations involving the hydrophobic methyl group are similar to the corresponding distributions computed by Pratt and Chandler for nonspherical apolar molecules in water (see Figs. 2, 3, and 4 of Ref. 45 and Fig. 3 of Ref. 46). For completeness, the re-

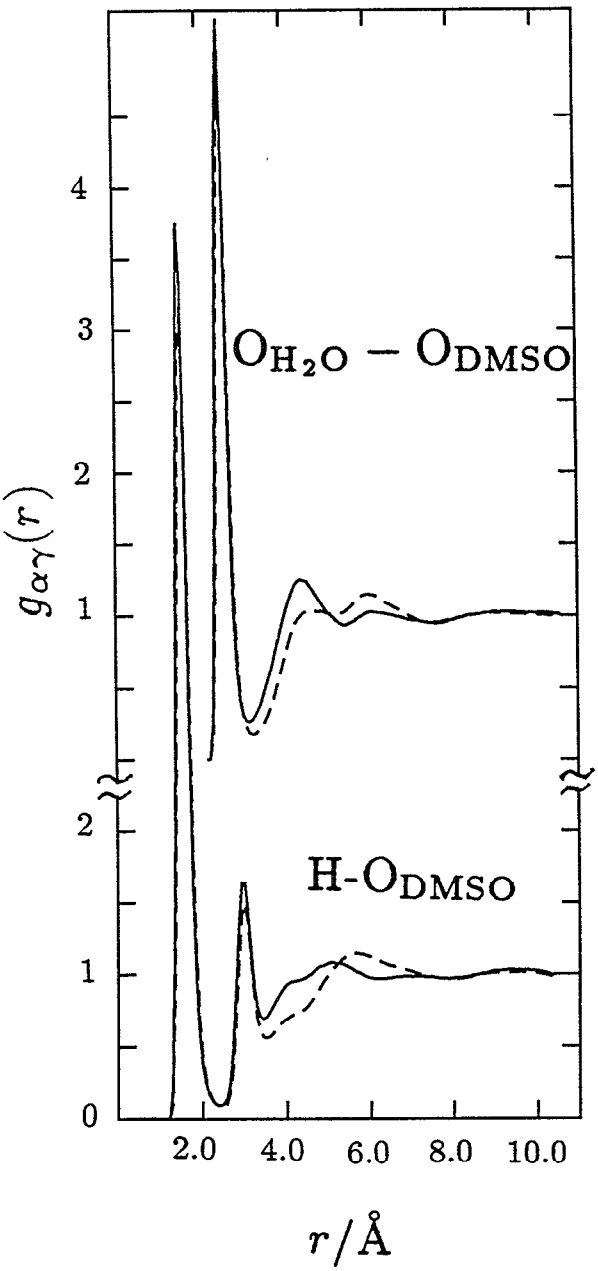

FIG. 3. Atom–atom pair distribution functions for water–DMSO mixture with $x_2=0.35$. Lines and lettering as in Fig. 1.

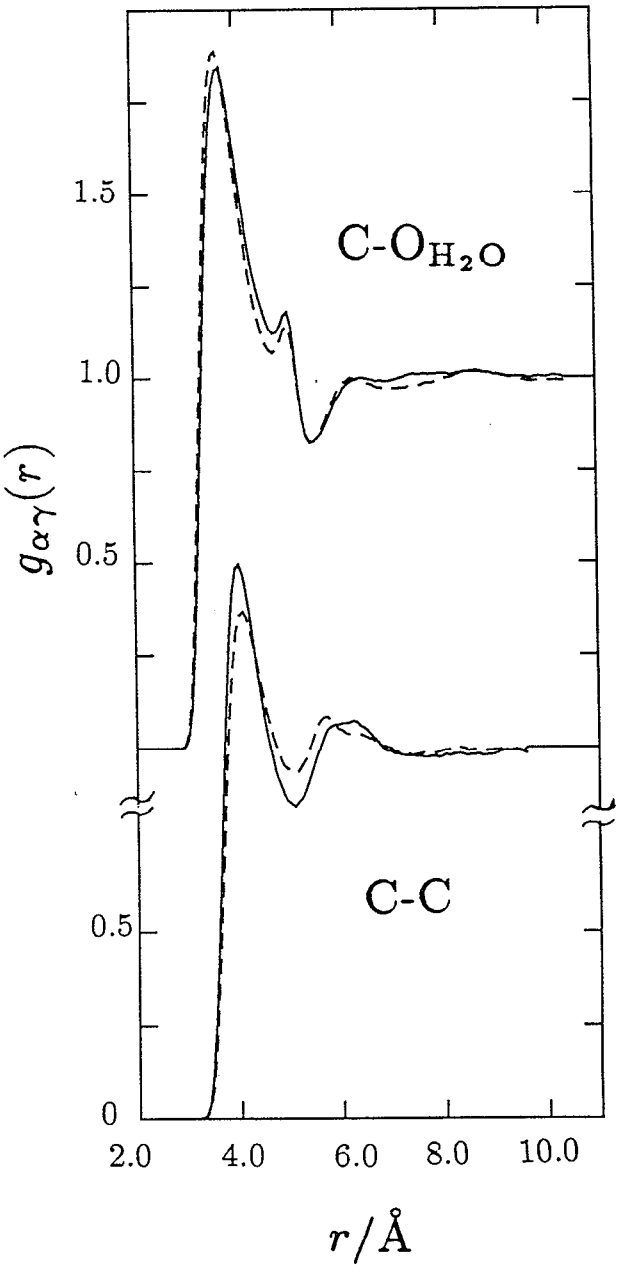

FIG. 4. Atom–atom pair distribution functions for water–DMSO mixture with $x_2=0.35$. Lines and lettering as in Fig. 1.

maining radial distribution functions are provided in Fig. 5. There, it is interesting to compare the C–H radial distribution in Fig. 5 with the corresponding $C\text{–}O_{H_2O}$ function plotted in Fig. 4. The sharpness and location of the main peak and cusped shoulder in the C–H function manifests the presence of orientational correlations in the hydrophobic solvation.

In Fig. 6, we present running coordination numbers

$$n_{\alpha\beta}(r)=4\pi\rho_\beta\int_0^r g_{\alpha\beta}(r')r'^2\,dr', \tag{3}$$

where ρ_β is the bulk number density of atom β. The hydration number could be defined as the plateau value of the running coordination number of the water oxygen. For both potential models, $n_{\alpha\beta}(r)$ increases continuously with distance. Hence, there is no well defined hydration shell of water around the sulfur atom of DMSO. This result is due, at least in part, to the steric hindrance of the methyl group which causes water molecules to associate with DMSO over a range of distances.

Consider now how the radial distribution functions of water molecules change with concentration of DMSO. Fig-

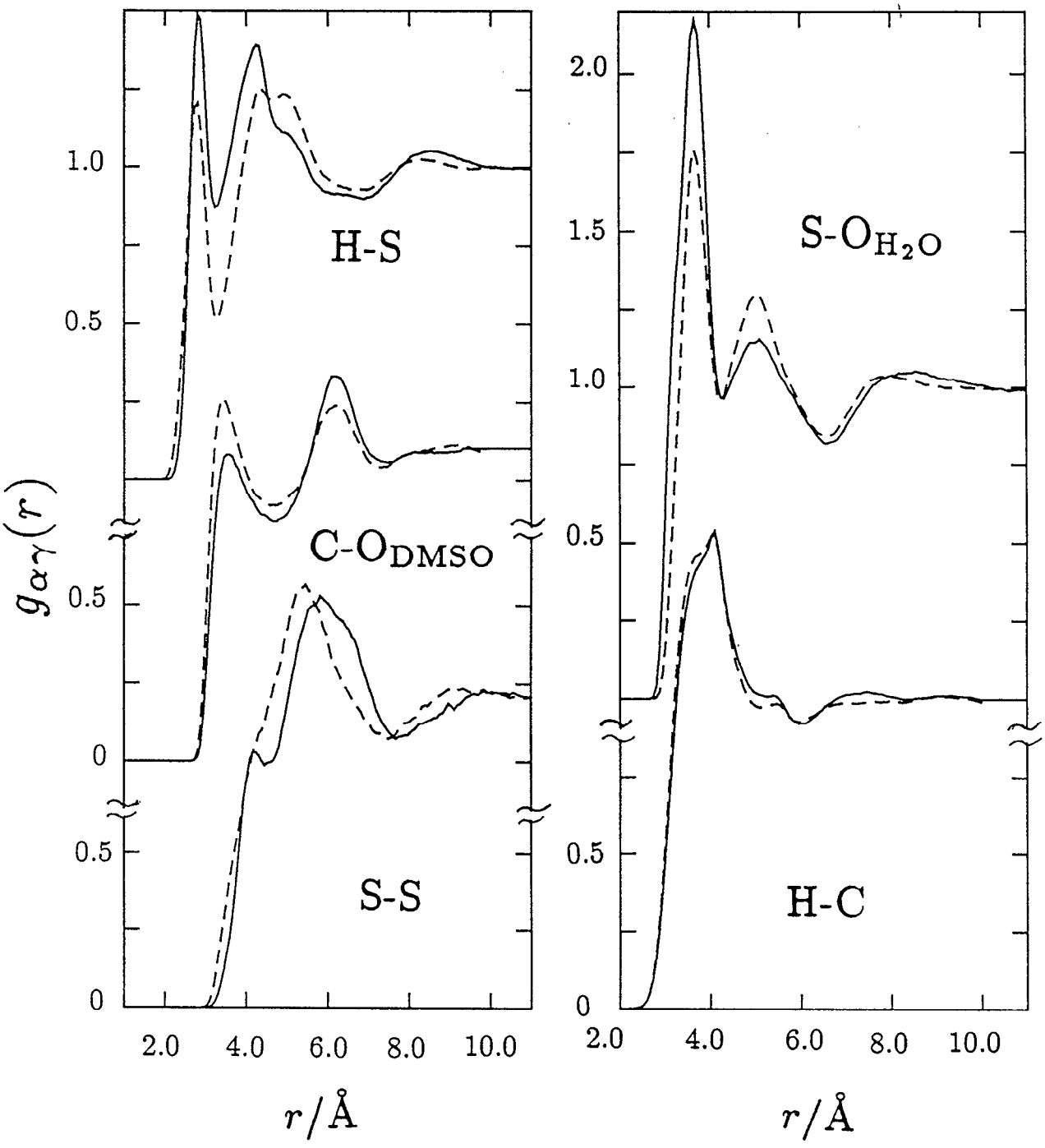

FIG. 5. Atom–atom pair distribution functions for water–DMSO mixture with $x_2=0.35$. Lines and lettering as in Fig. 1.

ure 7 shows the pair-distribution functions for water molecule oxygen atoms in 1:4 and 1:2 mixtures, as well as for pure SPC water. In this case we present results for P2 potential only. Both mixtures have their main O–O peaks at the same distance, but the peak intensities increase on going from pure water to 1:4 and 1:2 mixture. The same features are seen also in O–H distribution functions (Fig. 8), indicating the persistence of the hydrogen bonds, but also an increased first coordination shell structure at both compositions of the mixture. The same behavior of water radial distribution functions as a function of the solute concentration has been observed from MD simulation studies of water–methanol,[35] water–acetone,[35] water–ammonia,[35] and water–acetonitril[47] mixtures. It is evident from Figs. 7 and 8 that the nearest neighbor tetrahedral structure of water in the mixture is preserved. However, the decrease in net water density with increasing DMSO concentration causes the coordination numbers to decrease

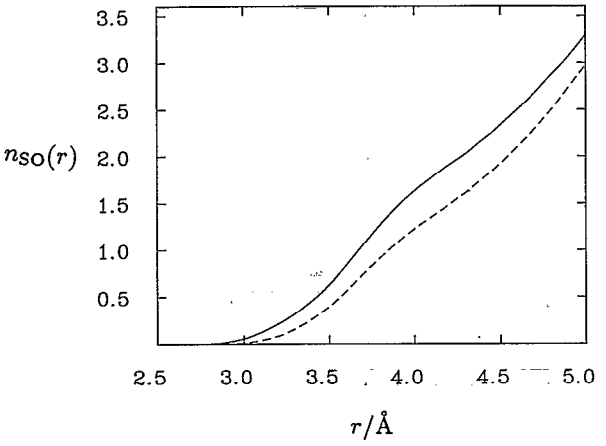

FIG. 6. Running coordination number, $n_{SO}(r)$ [Eq. (3)] for water oxygen atoms around DMSO sulfur atoms calculated using P1 (solid line) or P2 (dashed line) potentials for pure DMSO.

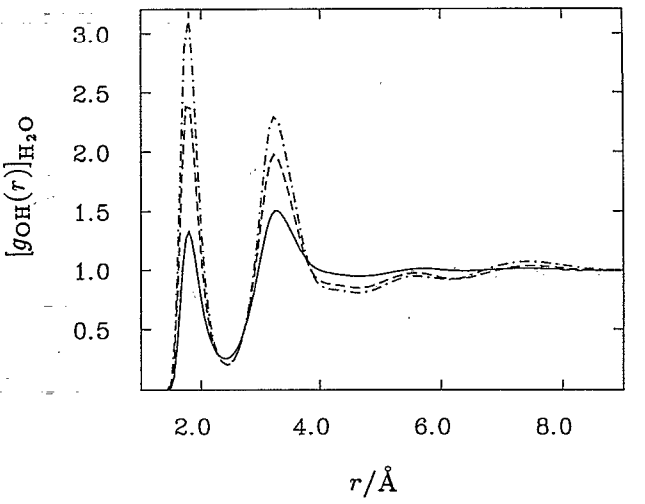

FIG. 8. Molecular dynamics results for oxygen–hydrogen radial distribution function of water. Lines as in Fig. 7.

with increasing mole fraction of DMSO in the system (Table III). Further, it is worth noting that the remaining water molecules are more strongly correlated with each other, therefore higher peaks in the radial distribution functions for water in the mixture (Figs. 7 and 8) are observed compared to pure water.

B. Comparison with neutron diffraction experiment[24] and mean-field model (MFM)[9]

In the case of aqueous solutions of DMSO, it is not possible to obtain a complete separation of all the partial correlation functions by isotropic contrast, because two of the scattering lengths of two of the components, oxygen and carbon, change little with isotope. Sulfur could be substituted, although a very weak contrast and also high cost inhibits its use. On the other hand, hydrogen and its isotope deuterium have a significant contrast. Because deuterium has a markedly different neutron scattering cross section from hydrogen, we can explore the distribution of hydrogen bonds in water and water mixtures by isotopic labeling of the protons involved in hydrogen bonding. As with most isotope difference techniques the H/D substitution yields partial structure factors to absolute accuracies of $\sim 10\%$. Within that accuracy, important trends with dilution and in comparison with pure water are detectable. In all the experiments, DMSO was fully deuterated to reduce the incoherent scattering as much as possible. In analyzing simulation data we will focus on the manifestation of DMSO induced changes in water–water interactions, as measured by neutron diffraction.[24]

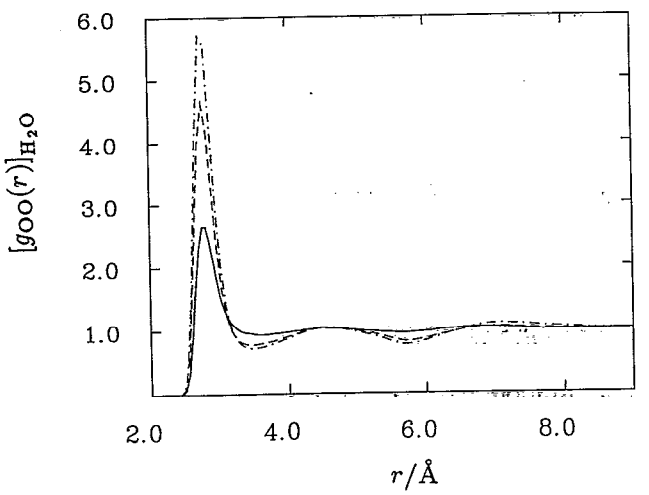

FIG. 7. Molecular dynamics results for the oxygen–oxygen radial distribution function of water in pure SPC (solid line), water in 1:4 mixture (dashed line) and water in 1:2 mixture (dashed–dotted line).

1. H–H correlations

In Figs. 9 and 10, molecular dynamics results are presented at two concentrations of the mixture and compared with neutron diffraction data.[24] Results for pure SPC are also included for comparison. There is no significant difference in hydrogen–hydrogen radial distribution function, $g_{HH}(r)$, calculated by the two potentials for DMSO. Therefore we cannot give preference to either of the two models on the basis of water pair correlation functions in

TABLE III. Coordination numbers, $n_{\alpha\beta}(r)$ [Eq. (3)] in pure water and aqueous solutions of DMSO determined by molecular dynamics simulation; x_1 denotes mole fraction of water.

	$x_1=1$	$x_1=0.79$	$x_1=0.65$
Oxygen around oxygen	5.92	3.35	2.60
Hydrogen around oxygen	1.84	1.42	1.16

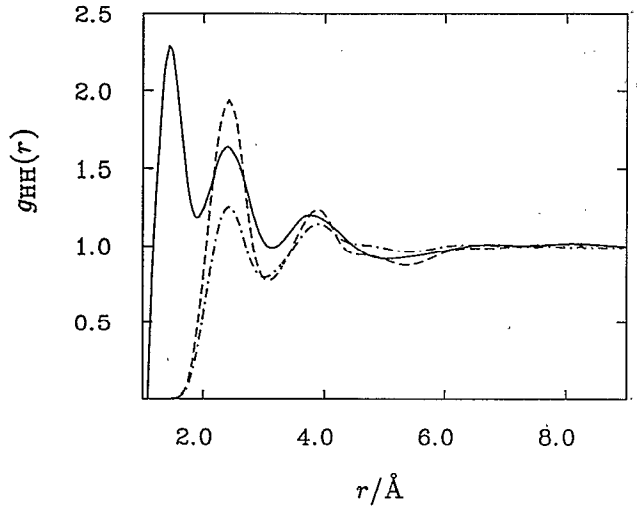

FIG. 9. H–H correlations in water–DMSO mixture at $x_2=0.21$. Solid line represents $g_{HH}(r)+s_{HH}(r)$ as determined by the neutron experiment (Ref. 24) where $s_{HH}(r)$ denotes intramolecular H–H distribution function. Dashed line is $g_{HH}(r)$ from molecular dynamics simulation (MD). On the scale of the graph, the distribution between MD calculations with potential model P1 are indistinguishable from those with P2. Dash–dot line represents molecular dynamics calculation of pure SPC water.

the mixture. The HH function in pure water is dominated by three peaks at 1.5, 2.3, and 3.8 Å. The latter two correspond to a mostly tetrahedral coordination of the water molecules. The peak at 1.5 Å corresponds to the intramolecular bond distance and is not interesting from the point of view of orientational correlations. If the positions of the intermolecular peaks change, or even merge into a single broad peak in the mixture, this would be an indication of a significantly distorted first molecular coordination shell

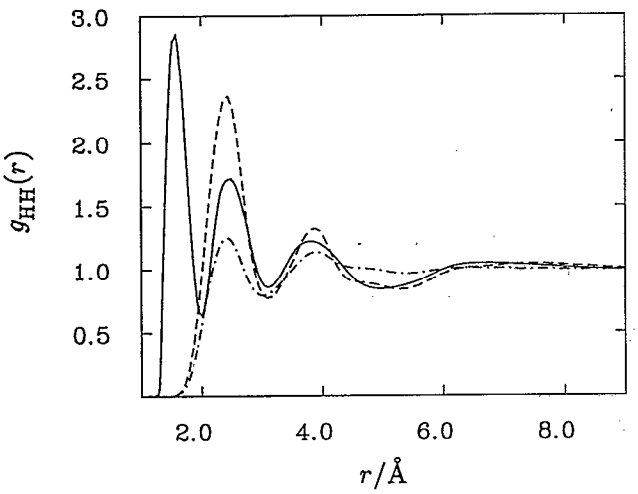

FIG. 10. H–H correlations in DMSO–water mixture at $x_{DMSO}=0.35$. Lines as in Fig. 9. Experimental uncertainties in the height of the first intermolecular peak, based upon two independent measurements (Refs. 24 and 58) are ±13%.

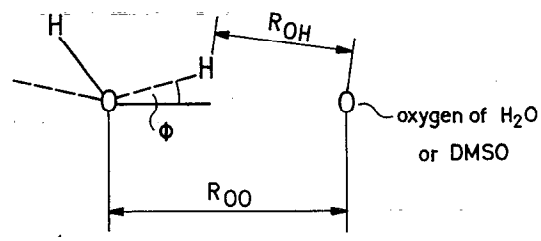

FIG. 11. Geometric definition of the hydrogen bond, used in molecular dynamics simulation.

structure in the mixture. This type of behavior is observed in concentrated ionic solutions of LiCl, for example,[48] but not in DMSO–water mixtures.

The 2.3 Å peak in pure water is shifted to slightly larger r values at the highest concentration of DMSO in the neutron diffraction experiment ($\Delta r\sim 0.15$ Å). No such shift has been detected in methanol–water mixtures or $CSCl_2$ water mixtures, however, a similar shift has been recently seen in pure water at elevated temperatures along the coexisting curve.[49] Molecular dynamics of the system we examined gives a negligible shift. The experimental shift of 0.15 Å is small enough to be due to quantum effects.[50] In making this comparison, note that the SPC model gives a $g_{HH}(r)$ for pure water whose phase is ~ 0.06 Å larger than that of experiment.[51] As seen from Figs. 9 and 10 there is no significant change in the general pattern in $g_{HH}(r)$ even at the highest concentration of DMSO. The H–H distributions obtained from simulations show more structure compared to neutron data. Notice, however, that the experimental intramolecular peak is somewhat broader than might seem physically reasonable thus indicating possible experimental uncertainties. Since the neutron data underestimates intramolecular correlations, it may also underestimate the intermolecular structure. This point is the focus of future experimental work.

In general, the qualitative trends seen in the experiment are also seen with the simulation: for the DMSO solutions the same sequence of peaks is observed, indicating that the most probable nearest neighbor tetrahedral coordination of water has not been significantly changed by the presence of concentrated DMSO. At those high concentrations of DMSO a significant fraction of water molecules will take part in the hydration shell of DMSO molecule. The first coordination shells exhibit progressively pronounced structure with increasing DMSO concentration. Correspondingly, the non nearest neighbor structure (i.e., the tetrahedral network of liquid water) must be diminished with increasing DMSO concentration.

2. Hydrogen bond structure

a. Hydrogen bond definition. To extend this analysis of the effect of DMSO on water structure, we use molecular dynamics to look at the hydrogen bond statistics as a function of mole fraction. The definition of a hydrogen bond is somewhat arbitrary. Different definitions have been used to

TABLE IV. Values of the parameters in Fig. 11. Their determination is explained in the text.

Mole fraction of DMSO	$R_{OO}^{(c)}$ (Å)	$R_{OH}^{(c)}$ (Å)	$\phi^{(c)}$/deg
0.00	2.45	3.60	30
0.21	2.40	3.20	30
0.35	2.40	3.20	30

estimate the number of hydrogen bonds of a given type on the basis of various energetic and structural criteria.[52] We have here adopted a geometric criterion similar to that used by Klein and co-workers regarding water–methanol and water–acetone mixtures.[35] We say that a hydrogen bond exists between a pair of molecules if the coordinates defined in Fig. 11 are smaller than some specified cutoff distance $R_{OO}^{(c)}$, $R_{OH}^{(c)}$, and angle $\phi^{(c)}$. We define the hydrogen bond occupation number for the αth pair of molecules to be

$$h_\alpha = 1, \quad \text{for} \quad R_{OO} < R_{OO}^{(c)},\ R_{OH} < R_{OH}^{(c)}, \text{ and } \phi < \phi^{(c)}$$
$$= 0, \quad \text{otherwise.} \tag{4}$$

The index α can refer to a water–water pair in pure water or in the mixture or a water–DMSO pair in the mixture. Our choices for the cutoff distances are taken to be the distance of the first minimum in the corresponding radial distribution functions, and they are listed in Table IV. Our choice for the cutoff angle, $\phi^{(c)}$, for water–water or water–DMSO pairs in the mixture is arrived at by studying the average number of hydrogen bonds, $\langle N_{1j}\rangle$, as a function of $\phi^{(c)}$. Here $j=1$ for water–water and $j=2$ for water–DMSO pair. In terms of the H-bond occupation number

$$\langle N_{1j}\rangle = \left\langle \sum_{\alpha\in j} h_\alpha \right\rangle, \tag{5}$$

where "$\alpha\in j$" indicates that the sum includes only $1j$ pairs. Figure 12 shows the behavior of $\langle N_{1j}\rangle$ as a function of

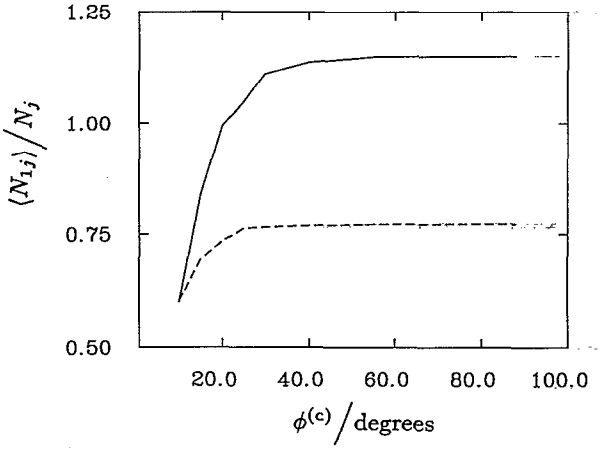

FIG. 12. The average number of water–water hydrogen bonds ($j=1$, solid line) and water–DMSO bonds ($j=2$, dashed line) per number of molecules, N_j, as a function of cutoff angle $\phi^{(c)}$ (defined in Fig. 11). These curves are for DMSO mole fraction 0.35.

$\phi^{(c)}$. The value we adopt, $\phi^{(c)}=\pi/6=30°$ (Table IV), is close to that where $\langle N_{1j}\rangle$ becomes almost invariant to $\phi^{(c)}$. The fact that a near invariance exists for relatively small $\phi^{(c)}$ is an indication of the directionality of the hydrogen bonds between water–water and water–DMSO in the mixture. The choice of $\phi^{(c)}=30°$ is the same as that adopted in Ref. 35 studying water–methanol and water–acetone interactions. For water–water interactions in pure water we retain the same value of $\phi^{(c)}$. A somewhat larger value of $\phi^{(c)}$ would account for nonlinear hydrogen bonds and bring our population criterion into quantitative accord with Jorgensen's *et al.*[53] energetic criterion for hydrogen bonding in pure water. Jorgensen finds 3.54 such bonds per water molecule, using SPC potential. We find 3.33 hydrogen bonds per water molecule with our choice of geometric criterion applied to pure water (Table V). We regard differences of this size to be unimportant to the analysis given here.

The distribution of the number of water–water hydrogen bonds per molecules of water in 1:4 and 1:2 mixture, compared to pure SPC is presented in Table V. The distribution of the number of water–DMSO hydrogen bonds per water molecule in the 1:4 and 1:2 mixtures are also presented in Table V. Note that the average number of water–water hydrogen bonds per water molecule decreases with the increasing DMSO concentration, as expected. It is also apparent from Table V, that the probability for DMSO to have three hydrogen bonds with water molecules is significantly less than compared to probabilities of having two or one hydrogen bonds at both concentrations studied.

b. Coordination numbers. A general scheme for analyzing experimental neutron diffraction data on the HH and OH pair correlation function in terms of coordination numbers has been proposed recently.[24] The approach utilizes a simple model, developed for calculating thermodynamic and interfacial properties of water[54,55] and water mixtures.[9–11] The model incorporates the effect of the strong orientation dependent hydrogen bond interaction in a mean-field approximation (MFM). The aqueous mixture is treated as an ensemble of a large number of pairs consisting of a proton on a water molecule and a hydrogen bonding site on an oxygen atom of water (species 1) or DMSO (species 2). Heuristically, one can think of these hydrogen bonding sites as locations of "lone pair electrons," recognizing that this terminology is a pneumonic representation, not a replacement of the actual intermolecular potentials that control the dynamics and structure of the system. The 11 and 12 pairs are able to form a hydrogen bond or are unable to do so depending on the local environment of the water molecule. For the pairs able to form a bond, there is an equilibrium between formed and broken bonds. It is assumed that a maximum of either two ($m=2$) or three ($m=3$) water molecules per one DMSO molecule can be formed. The total number density of pairs $n_{11}+n_{12}$ is set equal to $2n_1$, where n_1 is the number density of water molecules. This implies that all the protons in the solution are able to participate in a bond. The probabilities of a bond formation of $1i$ ($i=1$ for water, $i=2$ for DMSO), B_{1i}, depend on the composition of the mixture and are determined by Boltzmann statistics; $B_{1i}\equiv\exp(-\beta\Delta A^{1i})$,

TABLE V. Average fraction of water and DMSO molecules (%) with N hydrogen bonds at mole fraction of water, x_1; statistics is obtained from two independent 2.5 ps runs. Numbers in parentheses were computed at $x_1=0.65$ with the SPC and P1 potentials; all others were evaluated with the SPC and P2 potentials.

	$x_1=1$	$x_1=0.79$		$x_1=0.65$			
N	H_2O	H_2O	DMSO	H_2O		DMSO	
0	0.07±0.01	0.41±0.05	0.38±0.05	2.20±0.02	(4.03)	0.7±0.02	(1.43)
1	2.12±0.08	7.6 ±0.6	24.6 ±0.9	19.0 ±2.0	(22.9)	58.2±0.5	(44.1)
2	14.11±0.30	30.6 ±0.2	69.3 ±0.6	42.0 ±2.5	(42.6)	39.7±0.5	(54.4)
3	38.12±0.45	41.7 ±0.2	5.7 ±0.3	30.0 ±1.0	(26.5)	1.4±0.7	(0.05)
4	40.58±0.50	18.7 ±0.5	0.04±0.04	7.0 ±1.7	(4.0)	0.0	
5	4.93±0.15	1.0 ±0.1	0.0	0.2 ±0.1	(0.0)	0.0	
6	0.06±0.01	0.0	0.0	0.0	(0.0)	0.0	

where β^{-1} is temperature times Boltzmann's constant, and ΔA^{1i} is the free energy change due to the formation of $1i$ pair, able to form a bond, as defined in Ref. 10. The number density of water–DMSO pairs, n_{12} is obtained from

$$0=B_{11}\ln(1-n_{12}/mn_2)-B_{12}\ln(n_{12}/2n_1), \qquad (6)$$

where n_2 is the number density of DMSO molecules.

The phase space of $1i$ pairs is formally divided into two subvolumes: V_1^{1i} for hydrogen bonded and V_0^{1i} for nonhydrogen bonded pairs, with only two energy levels, E^{1i} ($i=1,2$) <0 for formed bonds, and zero otherwise. It is assumed that pairs unable to form a bond can adopt all possible points in phase space. The fraction of formed bonds ω^{1i} out of all pairs able to form a bond of a given type (11 or 12) is given by

$$\omega^{1i}=\frac{1}{1+\alpha^{1i}\exp(\beta E^{1i})}, \qquad (7)$$

where $\alpha^{1i}\equiv V_0^{1i}/V_1^{1i}$. Parameters of the model, the relative strength of the water–water and water–DMSO hydrogen bonds, E^{1i} and the entropies of the H-bond formation $\Delta S^{1i}=-kT\ln\alpha^{1i}$ were estimated from independent measurements: scattering data[56,57] and thermodynamic data.[5,6] With this approach the average number of hydrogen bonds per water molecule for $1i$ pairs, $\langle n_{HB}^{1i}\rangle = n_{1i}\omega^{1i}/n_1$ was calculated.[9]

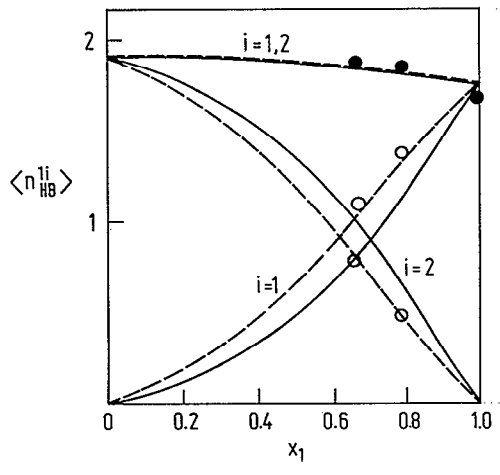

FIG. 13. Comparison of the average number of hydrogen bonds per water molecule, $\langle n_{HB}^{1i}\rangle$, ($i=1$ for water and $i=2$ for DMSO), as a function of the mole fraction of water, x_1, determined from mean-field model (Ref. 9) (solid lines for $m=3$, dashed lines for $m=2$), and by molecular dynamics simulation (open and filled circles).

We have computed $\langle n_{HB}^{11}\rangle$ and $\langle n_{HB}^{12}\rangle$ also by molecular dynamics. In our molecular dynamics calculations, $\langle n_{HB}^{1i}\rangle$ corresponds to $N_1^{-1}\langle N_{1i}\rangle$ where N_1 is the number of water molecules in the system. We place our molecular dynamics results on a graph showing the theoretical results taken form Ref. 9. This is done in Fig. 13. Notice that the sum, $\langle n_{HB}^{11}\rangle+\langle n_{HB}^{12}\rangle$, remains relatively constant independent of mole fraction of water. Notice too that the MD data agree very well with the model predictions for $m=2$. This remarkable agreement supports the assumption of the model that a hydrogen bond is lost for every direct association of a water molecule with a DMSO molecule.[9–11]

An important question, not answered definitively by the neutron diffraction experiments,[24] is whether the oxygen on DMSO molecule can possibly form two or three hydrogen bonds. It turns out that the neutron diffraction data are not very sensitive to the number of hydrogen bonding sites on the oxygen atom of DMSO (see Fig. 12 of Ref. 24). The same observation emerged from previous calculations[9–11] where it has been pointed out that the difference between the shapes of the theoretical thermodynamic curves was too small for any conclusion about the real number of hydrogen bonds between DMSO and water could be made. Neutron data and also our MD calculations (Fig. 13) show better agreement with $m=2$, while the previous analysis[9–11] gave slightly better agreement with thermodynamic experimental data for $m=3$. Hence, all these results are most consistent with the choice of $m=2$ and not 3 for the maximum possible number of hydrogen bonds formed with DMSO. Note that this is a quantitative detail and not a matter of qualitative trends. See Fig. 13. Further, as the histograms tabulated in Table V show, the distribution of hydrogen bond numbers change with concentration; at the highest concentrations of DMSO, the most probable solvation of DMSO can have fewer hydrogen bonds than the maximum of 2.

We have investigated how much the choice of potential for DMSO influences hydrogen bond distributions. Data

collected in Table V show that the P1 potential favors ~9% more hydrogen bonds between DMSO–water molecules compared to the P2 potential, and ~9% less hydrogen bonds between water-water molecules in 1:2 mixture. These differences between the two potentials are considered only partly to be due to statistical uncertainty. Hence, we have to bear in mind, that the population of hydrogen bonds between water–DMSO molecules in 1:2 mixture depends to some extent on the potential of DMSO used in simulations. Notice, for example, that the probability for two hydrogen bonds with DMSO is larger for the P1 potential model than that for the P2 potential model. This feature is understandable. The charge on the DMSO oxygen is smaller in the P2 potential than it is in the P1 potential. As a result, the DMSO–H_2O hydrogen bond is slightly weaker in the former case.

We now consider the structure of the DMSO–water hydrogen bonded aggregates. By molecular dynamics, we calculated the H···O–S angle. Its average value is $126°\pm2°$ for either of the two potentials. The assumption of a planar coordination of the DMSO oxygen atom therefore coincides with a tetrahedral angle between hydrogen bonds in the DMSO : $2H_2O$ aggregate. This structure is consistent with a relatively unperturbed local tetrahedral structure of water in the presence of DMSO, as observed by neutron diffraction.[24]

Table VI compares coordination numbers for selected peaks in HH and $H(O_{H_2O}+O_{DMSO})$ correlation functions, obtained from our molecular dynamics and from neutron diffraction experiments. These values are results of integrating the first intermolecular peak of the corresponding radial distribution functions. Table VI also gives O–H coordination numbers estimated from the mole fraction weighted averages of $\langle n_{HB}^{1i}\rangle$ predicted by the mean-field model of Ref. 9. Comparing the coordination numbers from H–H correlations, we see a diminishment of hydrogen bonds with increasing DMSO concentration, indicating that the water hydrogen bonding sites are becoming increasingly less hydrogen bonded with increasing concentration of DMSO. We observe the same phenomena in molecular dynamics and the neutron diffraction experiment. It is therefore evident that DMSO hydrogen bonds to water in preference to the water itself. Comparing the coordination numbers from $H-(O_{water}+O_{DMSO})$ correlations, the experiment, simulation and mean-field model all give almost the same number at the lower concentration of DMSO; however, at the highest concentration studied, neutron diffraction gives a questionably low value. This experiment has since been repeated and shows a slightly better agreement with our simulations and the mean field model, the revised coordination number being 1.7 ± 0.2.[58] The neutron diffraction results for coordination numbers are difficult to obtain in part because they are subject to seemingly small errors in the background subtraction. Also, neutron diffraction has not distinguished between the two types of OH correlations. To obtain these coordination numbers from neutron diffraction, it was assumed that H's were equally distributed between DMSO and H_2O. However, the general trend is visible in the experiment: The water–water bonds are depleted as the increasing concentration of DMSO absorbs the water hydrogens.

TABLE VI. H–H and $H-(O_{water}+O_{DMSO})$ coordination numbers in DMSO–water mixtures; comparison between neutron diffraction (ND) (Ref. 24) molecular dynamics (MD) (this work), and mean field model (MFM) (Ref. 9). The integration ranges for the calculation of coordination numbers are in parentheses. Distances are in Angstroms.

	HH correlations			
Mole fraction of DMSO	ND		MD	
0.21	1.3±0.1	(1.9–2.40)	1.63	(1.88–2.423)
	4.2±0.1	(1.9–3.10)	4.2	(1.88–3.10)
0.35	0.9±0.1	(2.00–2.45)	1.22	(2.01–2.44)
	2.6±0.1	(2.00–3.10)	3.00	(2.01–3.09)

	$H-(O_{water}+O_{DMSO})$ correlations				
Mole fraction of DMSO	ND		MD		MFM
0.21	1.4±0.1	(1.4–2.20)	1.41	(1.40–2.20)	1.45
0.35	0.7±0.2	(1.40–2.30)	1.21	(1.40–2.3)	1.15

IV. HYDROGEN BOND DYNAMICS

The preceding section discussed the equilibrium properties of the hydrogen bonds in the mixture. Equally interesting is the question of the time-dependent behavior of the bonds, one measure of which is the hydrogen bond lifetime.

There have been some efforts at using simulation results to study lifetimes in a way proposed by Stillinger[59] nearly 20 years ago for water, however, in only a few studies reported, time dependent hydrogen bond autocorrelation functions were actually computed.[60–63] In systems where we expect relatively long lifetimes, as in the case of DMSO–water mixtures, the direct determination of the hydrogen bond autocorrelation function seems less efficient than the reactive flux method often used in the context of isomerization dynamics.[26,27] The reactive flux method provides information about the short time dynamics, i.e., transient relaxation, as well as the lifetime. It is this approach that we adopt here.

Let us define a hydrogen bond correlation function $c_{1j}(t)$ as

$$c_{1j}(t)=\frac{1}{\langle N_{1j}\rangle}\left\langle \sum_{\alpha\in j}[\delta h_\alpha(0)\delta h_\alpha(t)]\right\rangle, \tag{8}$$

where $j=1$ for water and $j=2$ for DMSO and the dynamical variable $h_\alpha(t)=\delta h_\alpha(t)+\langle h_\alpha\rangle$ is defined in Eq. (4). The sum in Eq. (8) is taken over all pairs consistent with the index j and $\langle\cdots\rangle$ represents the average over initial times. Note that $c_{1j}(t)$ as defined in Eq. (8) has the initial, $t=0$, value of unity. By assuming exponential relaxation beyond a transient time, we would write

$$c_{1j}(t)=e^{-t/\tau}, \quad \text{for} \quad t>t_{\text{transient}}, \tag{9}$$

where τ is the relaxation time for times longer than that of the transient. Taking the time derivatives of Eqs. (8) and (9), we obtain

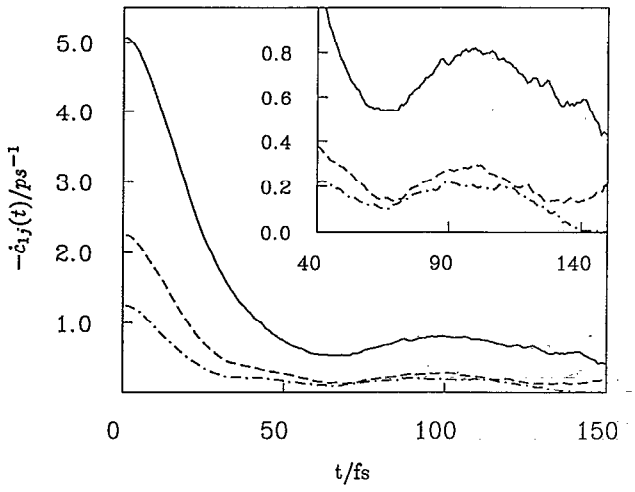

FIG. 14. Hydrogen bond autocorrelation function derivative $-\dot{c}_{ij}(t)$, calculated by molecular dynamics; solid line denotes $-\dot{c}_{11}(t)$ for water–water pairs in pure water; dashed line and dash–dot line denote $-\dot{c}_{11}(t)$ and $-\dot{c}_{12}(t)$, respectively, for water–water and water–DMSO pairs in the mixture with mole fraction of DMSO, $x_2=0.35$.

$$-\dot{c}_{1j}(t)=\frac{1}{\langle N_{1j}\rangle}\left\langle \sum_{\alpha\in j}\dot{h}_\alpha(0)h_\alpha(t)\right\rangle=\frac{1}{\tau}e^{-t/\tau}, \quad (10)$$

where the dot denotes the time derivative. By employing the reactive flux method, we can inspect the consistency of this exponential model for long time relaxation.

For short times we expect transient behavior that should not correspond to the exponential macroscopic decay. The initial value of $-\dot{c}_{1j}(t)$ determines the transition state theory relaxation time, τ_{TST}. After a relatively short transient time, $-\dot{c}_{1j}(t)$ should relax to a plateau value corresponding to a long time behavior, determining the hydrogen bond lifetime, τ_{HB}. Short time behavior provides information about the mechanism for hydrogen bond breaking. But its particular functional form is sensitive to the particular (and somewhat arbitrary) choice that we make for the hydrogen bond. Exponential relaxation on a longer time scale, however, should be invariant to the definition of the hydrogen bond, provided a reasonable choice for that bond has been made.

In Fig. 14, $-\dot{c}_{1j}(t)$ is presented for water–water pair ($j=1$) and water–DMSO pair ($j=2$) in a 2 H_2O: 1 DMSO mixture and compared with pure water at $T=289$ K. The analysis in the mixture was carried out for 0.2 ps covering different portions of the simulations, and the results averaged over 50 runs, with time step of 1.0 fs and using P2 potential for DMSO. The analysis in pure water, using SPC potential, was carried out for 0.4 ps (time step=0.05 fs), and the results averaged over 25 runs. The derivatives of the autocorrelation functions were calculated every time step. Our calculations of $-\dot{c}_{1j}(t)$ are consistent with a rapid transient relaxation. The simulation runs were, however, not long enough to show clearly whether the plateau has been reached, and if it existed, to determine an accurate plateau value of $-\dot{c}_{ij}(t)$. This is left for future work. Present calculations (Fig. 14) indicate that the recrossings lead to relaxation times which are almost an order of magnitude longer than those obtained from the transition state theory. Further, oscillations in $-\dot{c}_{ij}(t)$ show that the recrossing frequency is of the order of $(0.1\ \text{ps})^{-1}$. We use the value of $-\dot{c}_{ij}(t)$ after the end of the first recrossing period to estimate the transmission coefficient,[26] τ_{TST}/τ_{HB}, and therefore the hydrogen bond lifetime, τ_{HB}. The hydrogen bond lifetimes, extracted from the results depicted in Fig. 14 and considering Eq. (10) are collected in Table VII. Both the initial transition state theory as well as the dynamical values obtained from $-\dot{c}_{ij}(t)$ at $t=0.1$ ps are given. Our result for τ_{HB} in pure water is reasonably consistent with those found by others performing molecular dynamics with different potentials and techniques: 1.4;[64] 1.6;[62] 0.9,[35] and 2.0 ps.[65] Experimental estimates of hydrogen bond lifetimes made from interpreting depolarized Rayleigh light scattering and inelastic neutron scattering give $\sim$0.8 ps at room temperature.[64–69] Recall that it is only the complete breaking and making of hydrogen bonds that is analyzed with the plateau value of $-\dot{c}_{ij}(t)$. On the other hand, the line widths of the scattering experiments probably possess contributions from the dephasing of small amplitude librations in addition to the larger amplitude hydrogen bond fluctuations. As such, we expect the scattering experiments should yield a somewhat larger relaxation rate or a smaller relaxation time than the τ_{HB} we have computed.

TABLE VII. Hydrogen bond lifetimes, τ_{HB}, and the transition state theory estimate of that time τ_{TST}, for water–water pairs in pure water, water–water pairs in 1:2 mixture, and water–DMSO pairs in 1:2 mixture, extracted from Fig. 14, considering Eq. (10). For DMSO, the P2 potential was used. Calculations were done at $T=298$ K.

	τ_{TST}/ps	τ_{HB}/ps
Water–water pair in pure SPC	0.20±0.01	1.20±0.08
Water–water pair in 1:2 DMSO–water mixture	0.45±0.03	3.3 ±0.3
Water–DMSO pair in 1:2 DMSO–water mixture	0.80±0.06	4.8 ±0.9

One interesting feature of the entries to Table VII is that the transmission coefficient is approximately 1/6 for all three cases investigated. Our preliminary study would therefore indicate that the dynamical corrections to the statistical transition state theory are not strongly dependent upon either the type of hydrogen bond nor the concentration of DMSO. The larger value of τ_{HB} for the water–DMSO bond than for the water–water bond in the mixture is therefore understood as a simple statistical consequence of the former's hydrogen bond being stronger than the latter. Similarly, the increase of the water–water τ_{HB} through the addition of DMSO is understood statistically as the potential of mean force for water–water hydrogen bonding grows with increasing DMSO concentration (see Figs. 7, 8, and 10).

The tendency of water motion to progressively slow

with the increase in DMSO concentration is consistent with Baker and Jonas' NMR observations of both self-diffusion constant and the single molecule reorientational relaxation time, τ_θ, for water molecules in water–DMSO mixtures.[21] According to their data, $\tau_\theta \approx 3$ ps for pure water and $\tau_\theta \approx 11.7$ ps for the 2:1 water–DMSO mixture. (These numbers are extrapolated and interpolated from Table II in Ref. 21.) Our corresponding computed values of τ_{HB} are 1.2 and 3.3 ps, respectively. Consistency therefore implies that the reorientation of a water molecule by an angle $\sim\pi/2$ occurs in about three to four hydrogen bond lifetimes. Wang and co-workers[70] have used depolarized light scattering to estimate τ_θ for the DMSO molecules in water–DMSO mixture. At conditions coinciding with our simulation, they find τ_θ to be between 12 and 14 ps, again approximately three times the corresponding τ_{HB} which we have computed, 4.8 ± 0.9 ps. A recent NMR measurement to estimate τ_θ for water in the 2:1 water–DMSO mixture by Gordalla and Zeidler[19(b)] gives a value of 16.8 ps, about 30% larger than that of Barker and Jonas'.[21] The trends are consistent, though a precise connection between τ_θ and τ_{HB} has yet to be analyzed. Molecular dynamics calculations of τ_θ would be worthwhile and instructive in this regard.

V. CONCLUSIONS

With either potential model P1 or P2, our molecular dynamics results draw a consistent microscopic picture of water–DMSO mixtures. This robust picture, seemingly invariant to reasonable changes to the intermolecular potential, is in accord with the qualitative ideas underlying the mean-field model of those systems.[9–11] In particular, in the mixing process, hydrogen bonding is simply transferred from water–water interactions to water–DMSO interactions.

The radial distribution functions we have computed are in reasonable agreement with those observed with neutron diffraction.[24] Certain radial distribution functions, such as the water–water $g_{HH}(r)$, provide a signature of hydrogen bonding. We find that the peak locations in $g_{HH}(r)$ are hardly affected by DMSO. However, the peak amplitudes are altered significantly as the concentration of DMSO changes. Specifically, we find that the first molecular coordination shells become more structured with the increase of DMSO. At the same time, the average number of water–water hydrogen bonds diminish with increasing DMSO concentration thus signaling a disruption of the hydrogen bond network beyond the range of nearest molecular neighbors.

In a fluid mixture, average populations depend upon both the relative concentrations of the components as well as the pair correlations. The latter, of course, are described by the potentials of mean force, or equivalently the deviations of the radial distributions from unity. Hence, our simultaneous observations of diminishing number of water–water hydrogen bonds and increasing water–water correlations are not inconsistent. Indeed, without the increased correlations, the water–water bonding populations would decrease even faster than they do with increasing DMSO concentration.

The DMSO molecules create these structural effects in part because DMSO is a hydrogen bond acceptor but not donor, and in part because DMSO bonds with water more strongly than water bonds to water. According to the simulations, the solvated DMSO is likely bonded to two waters, and the average angle between the two hydrogen bonds in the DMSO :$2H_2O$ aggregate is nearly tetrahedral. A water is hydrogen bonded to water but near the oxygen of a DMSO molecule can simultaneously bond with DMSO or readily switch its bonding from water to DMSO. On the other hand, if that water was instead near the methyl groups of the DMSO, no such alternative bonding would be possible. It is the occurrence of this latter case that strengthens the attractive potential of mean force between pairs of waters in the presence of DMSO.

Our analysis of hydrogen bond lifetimes suggests that the slowing of water motions in the presence of DMSO can be understood as a consequence of these structural effects. Much more could be done to extend our preliminary work on the dynamics. First, more accurate estimates of the hydrogen bond lifetimes are needed. Runs with longer trajectories should provide quantitative plateau values of the reactive flux correlation functions have been reached. Further, the connections we have begun to make here between orientational correlation times and hydrogen bond lifetimes deserve quantitative elaboration. Analysis of the transient relaxations we have reported in Fig. 14 may be useful in furthering our understanding of water motion and the dynamics of solvation. Here we have in mind the possible development of analytical models that could be tested through comparison with the simulation results for $-\dot{c}_{1j}(t)$.

Concerning equilibrium structural aspects of this system, DMSO can serve as a prototypical amphiphilic molecule from which much may yet be learned about hydrophobic effects. Indeed, at lower DMSO concentrations that we have studied, Vaisman and Berkowitz[25] have contrasted the hydration of the hydrophilic S–O group from that of the hydrophobic CH_3 groups. Not all of the atom–atom distribution functions we have computed are accessible experimentally. However, through H/D substitution of the methyl hydrogens, it should be possible to use neutron diffraction to test our results involving the hydrophobic methyl groups. We hope that such experiments will be performed.[71]

ACKNOWLEDGMENTS

We thank Joel Bader, Massimo Marchi, and Berend Smit for their help and advice. The authors acknowledge valuable discussions with Alan Soper and José Teixeira. We thank Max Berkowitz for sending us the preprint of Ref. 25. This work was supported by NIH Grant No. R01 GM 37307 and ONR Grant No. N00014-92-J-136.

[1] D. Martin and H. G. Hauthal, *Dimethyl Sulphoxide* (Wiley, New York, 1975).

[2] D. H. Rasmussen and A. P. Mackenzie, Nature (London) **220**, 1315 (1968).
[3] M. Y. Doucet, F. Calmes-Perault, and M. T. Durand, C. R. Acad. Sci. **260**, 1878 (1965).
[4] E. Tommila and A. Pajunen, Suom. Kemistil. B **41**, 172 (1969).
[5] J. M. G. Cowie and P. M. Toporowski, Can. J. Chem. **39**, 2240 (1964).
[6] H. L. Clever and S. P. Pigott, J. Chem. Thermodyn. **3**, 221 (1971).
[7] M. F. Fox and K. P. Whittingham, J. Chem. Soc. Faraday Trans. **75**, 1407 (1974).
[8] J. Kenttammaa and J J. Lindberg, Suom. Kemistil. B **33**, 32 (1960).
[9] A. Luzar, in *Interactions of Water in Ionic and Nonionic Hydrates*, edited by H. Kleeberg (Springer, Berlin, 1987), pp. 125–129.
[10] A. Luzar, J. Chem. Phys. **91**, 3603 (1989).
[11] A. Luzar, in *Hydrogen–Bonded Liquids*, edited by J. C. Dore and J. Teixeira, NATO ASI Series (Kluwer Academic, Dordrecht, 1991), Vol. 329, pp. 197–210.
[12] A. Luzar, J. Mol. Liquids **46**, 221 (1990).
[13] G. J. Safford, P. C. Schaffer, P. S. Leung. G. F. Doebbler, G. W. Brady, and E. F. X. Lyden, J. Chem. Phys. **50**, 2140 (1969).
[14] M. Madigosky and R. W. Warfield, J. Chem. Phys. **78**, 1912 (1983).
[15] J. J. Lindberg and C. Majani, Acta Chem. Scand. **17**, 1477 (1963).
[16] J A. Glasel, J. Am. Chem. Soc. **92**, 372 (1970).
[17] A. Bertulozza, S. Bonora, M. A. Battaglia, and P. Monti, J. Raman Spectrosc. **8**, 231 (1979).
[18] G. Brink and M. Falk, J. Mol. Struct. **5**, 27 (1970).
[19] (a) B. C. Gordalla and M. D. Zeidler, Mol. Phys. **59**, 817 (1986). (b) **74**, 975 (1991).
[20] T. Tukouhiro, L. Menafra, and H. H. Szmant, J. Chem. Phys. **61**, 2275 (1974).
[21] E. S. Barker and J. Jonas, J. Phys. Chem. **89**, 1730 (1985).
[22] A. K. Soper and P. A. Egelstaff, Mol. Phys. **42**, 399 (1981).
[23] J. L. Finney, in Ref. 6, pp. 147–165.
[24] A. K. Soper and A. Luzar, J. Chem. Phys. **97**, 1320 (1992).
[25] I. I. Vaisman and M. L. Berkowitz, J. Am. Chem. Soc. **114**, 7889 (1992).
[26] D. Chandler, J. Stat. Phys. **42**, 49 (1986).
[27] D. Chandler, J. Chem. Phys. **18**, 2959 (1978).
[28] D. Chandler, *Introduction to Modern Statistical Mechanics* (Oxford, New York, 1987), pp. 242–246.
[29] H. J. C. Berendsen, J. P. M. Postma, W. F. van Gusteren and J. Hermans, in *Intermolecular Forces*, edited by B. Pullman (Reidel, Dordrecht, 1981).
[30] B. G. Rao and U. C. Singh, J. Am. Chem. Soc. **112**, 3803 (1990).
[31] We performed molecular dynamics runs on the pure liquid DMSO with molecular mechanics force field (Ref. 32) used in Refs. 25 and 30. We found, for example, that this force field gives a mean potential energy, $\langle U\rangle$, which is 30% lower than the experimental value (Ref. 33). The pressure computed from the virial theorem is very small, as it should be. Earlier simulations of DMSO systems (Refs. 25 and 30) were performed with truncated potentials. Our calculations utilized Ewald summation for electrostatic interactions and tail corrections for the Lennard-Jones potentials.
[32] N. A. Allinger and J. Kao, Tetrahedron **32**, 529 (1976).
[33] T. B. Douglas, J. Am. Chem. Soc. **70**, 2001 (1948); [the mean potential energy per mole, $\langle U\rangle$, was compared with the experimental value of the molar vaporization ethalpy, ΔH_v: $\langle U\rangle \sim -(\Delta H_v - RT)$, where RT has its usual meaning].
[34] J. P. Hansen and I. R. McDonald, *Theory of Simple Liquids*, 2nd ed. (Academic, London, 1986), p. 179.
[35] M. Ferrario, M. Haughley, I. R. McDonald, and M. L. Klein, J. Chem. Phys. **93**, 5156 (1990).
[36] R. Thomas, C. B. Shoemaker, and K. Eriks, Acta. Cryst. **21**, 12 (1966).
[37] H. L. Schlafer and W. Scheffernicht, Angew. Chem. **72**, 618 (1960).
[38] A. K. Soper, A. Luzar, and D. Chandler (to be reported).
[39] U. C. Singh and P. A. Kollman, J. Comput. Chem. **5**, 129 (1984).
[40] S. Nosé, J. Chem. Phys. **81**, 511 (1984).
[41] W. G. Hoover, Phys. Rev. A **31**, 1695 (1985).
[42] M. P. Allen and D. J. Tildesley, *Computer Simulation of Liquids* (Clarendon, Oxford, 1987).
[43] N. E. Dorsey, *Properties of Ordinary Water Substance* (Reinhold, New York, 1940), pp. 258, 574.
[44] C. A. Angell, M. Oguni, and W. J. Sichina, J. Chem. Phys. **86**, 998 (1982).
[45] L. R. Pratt and D. Chandler, J. Chem. Phys. **73**, 3430 (1980).
[46] L. R. Pratt and D. Chandler, in *Biomembranes, Protons and Water Structure and Translocation*, Methods of Enzymology, Vol. 127, edited by L. Packer (Academic, Orlando, 1986), pp. 48–63.
[47] H. Kovacs and A. Laaksonen, J. Am. Chem. Soc. **113**, 5596 (1991).
[48] R. H. Tromp, G. W. Neilson, and A. K. Soper, J. Chem. Phys. **96**, 8460 (1992).
[49] A. K. Soper (private communication).
[50] R. A. Kuharski and P. J. Rossky, J. Chem. Phys. **82**, 5164 (1985).
[51] A. K. Soper and M. G. Phillips, Chem. Phys. **107**, 47 (1986).
[52] M. Mezei, Phys. Many-body Systems **19**, 37 (1991).
[53] W. L. Jorgensen, J. Chandrasekhar, J. P. Madura, R. W. Impey, and M. L. Klein, J. Chem. Phys. **79**, 926 (1983).
[54] A. Luzar, S. Svetina, and B. Zeks, Chem. Phys. Lett. **96**, 485 (1983).
[55] A. Luzar, S. Svetina, and B. Zeks, J. Chem. Phys. **82**, 5146 (1985).
[56] W. A. P. Luck, Discuss. Faraday Soc. **43**, 115 (1967).
[57] G. E. Walrafen, M. R. Fisher, M. S. Hokmahadi, and W. H. Yang, J. Chem. Phys. **85**, 6970 (1986).
[58] A. K. Soper (private communication).
[59] F. H. Stillinger, Adv. Chem. Phys. **31**, 1 (1975).
[60] D. C. Rapaport, Mol. Phys. **50**, 1151 (1983).
[61] D. Bertolini, M. Casseratti, and G. Salvetti, J. Chem. Phys. **78**, 365 (1983).
[62] D. A. Zichi and P. J. Rossky, J. Chem. Phys. **84**, 2814 (1986).
[63] M. Matsumoto and K. E. Gubbins, J. Chem. Phys. **93**, 1981 (1990).
[64] F. Sciortino, P. H. Poole, H. E. Stanley, and S. Havlin, Phys. Rev. Lett. **64**, 1686 (1990).
[65] F. Sciortino and S. L. Formli, J. Chem. Phys. **90**, 2786 (1989).
[66] C. J. Montrose, J. A. Bucaro, J. Marshall-Coakley, and T. A. Litovitz J. Chem. Phys. **60**, 5025 (1974).
[67] W. Danninger and G. Zundel, J. Chem. Phys. **74**, 2769 (1981).
[68] O. Conde and J. Teixeira, J. Phys. (Paris) **44**, 525 (1983).
[69] S. H. Chen and J. Teixeira, Adv. Chem. Phys. **64**, 1 (1986).
[70] Y. Higashigaki, D. H. Christensen, and C. H. Wang, J. Phys. Chem. **85**, 2531 (1981).
[71] A. K. Soper and A. Luzar (to be reported).